Topside Plasma Flows in the Equatorial Ionosphere and their Relationships to F-Region Winds near 250 km

Roderick A. Heelis[1], Yun-Ju Chen[1], Matthew Depew[2], Brian J Harding[3], Thomas J. Immel[4], Stephen B Mende[4], Yen-Jung Joanne Wu[4], Joseph Huba[5], Christoph R Englert[6], Andrew W. Stephan[7], U. Kamaci[8], and Farzad Kamalabadi[9]

[1]University of Texas at Dallas
[2]Unknown
[3]UC Berkeley
[4]University of California, Berkeley
[5]retired, formerly NRL
[6]Naval Research Laboratory
[7]U.S. Naval Research Laboratory
[8]University of Illinois
[9]University of Illinois at Urbana Champaign

November 21, 2022

Abstract

Simultaneous measurements of F-region neutral winds near 250 km and topside interhemispheric plasma flow near 600 km, made by the ICON satellite, allow the connection between these parameters to be observationally established for the first time. The largest variations in the topside plasma flows are seen as a function of season and are shown to depend on trans-equatorial neutral winds below the F peak in a manner that is essentially the same during the daytime and the nighttime for the solar minimum conditions that prevail in 2020. This finding is consistent with established principles of a servo model of the ionosphere for which both production and loss rates in the topside are specified by the O/N_2 ratio at the F-peak height. The intermediate relationships, describing how the neutral wind influences the F-peak height and how the O^+ plasma pressure gradient across the equator influences the interhemispheric plasma flow are also investigated and found to be consistent with expectations.

R.A. Heelis[1], Y.-J. Chen[1], M.D. Depew[1], B.J. Harding[2], T.J. Immel[2], Y.-J Wu, S.B. Mende[2], J.D. Huba[3], C.R. Englert[4], A.W. Stephan[4], U. Kamaci[5], F. Kamalabadi[5]

1. William B. Hanson Center for Space Sciences, University of Texas at Dallas, Richardson, Texas

2. Space Sciences Laboratory, University of California Berkeley, Berkeley, CA

3. Syntek Technologies Inc., Fairfax, VA

4. Space Science Division, U.S. Naval Research Laboratory, Washington, DC

5. University of Illinois, Champagne, Urbana, IL

Corresponding author: Roderick Heelis (heelis@utdallas.edu)

Key Points:

Meridional winds below F-peak directly drive F-peak height and topside interhemispheric plasma flows

Transequatorial neutral wind at the magnetic equator linearly related to transequatorial plasma flow at the magnetic equator

ICON satellite provides the first observations of F-region winds and topside interhemisphere plasma flows.

Abstract

Simultaneous measurements of F-region neutral winds near 250 km and topside interhemispheric plasma flow near 600 km, made by the ICON satellite, allow the connection between these parameters to be observationally established for the first time. The largest variations in the topside plasma flows are seen as a function of season and are shown to depend on trans-equatorial neutral winds below the F peak in a manner that is essentially the same during the daytime and the nighttime for the solar minimum conditions that prevail in 2020. This finding is consistent with established principles of a servo model of the ionosphere for which both production and loss rates in the topside are specified by the O/N_2 ratio at the F-peak height. The intermediate relationships, describing how the neutral wind influences the F-peak height and how the O^+ plasma pressure gradient across the equator influences the interhemispheric plasma flow are also investigated and found to be consistent with expectations.

Plain Language Summary

Neutral winds in the upper atmosphere apply collisional forces to the charged particles that produce motions parallel and perpendicular to the magnetic field. Motions parallel to the magnetic field influence the distribution of charged particle pressure and thus change the plasma motion everywhere along the magnetic field. Simultaneous measurements of the neutral winds and the plasma motions at remote locations connected by the magnetic field allow the relationships between these quantities to be observationally established for the first time. These relationships show the direct relationships between the meridional winds near 250 km, the peak height of the ionospheric density and the interhemispheric plasma transport velocity at the apex of the magnetic field near 600 km.

1 Introduction

The plasma density in the topside low and middle latitude ionosphere is strongly influenced by dynamics and charge exchange chemistry. The charge exchange chemistry is a strong determinant of the relative contributions of O+ and H+, which are dependent on altitude, and at low levels of solar activity, can be important considerations above 500 km during the daytime and the nighttime (Heelis et al., 2009). In addition to the chemistry, are plasma motions parallel and perpendicular to the magnetic field. At low and middle latitudes, plasma motions perpendicular to the magnetic field are largely influenced by the dynamo action of neutral winds in the E-region and the F-region (Maute et al., 2012). The variability in the wind systems and the conductivity distribution in the E-region present a challenge to uncovering the most effective thermospheric oscillations that influence the F-region plasma motion. However, the recent availability of observations of neutral winds, plasma density and plasma velocity from the Ionospheric Connections (ICON) mission (Immel et al., 2018) have enabled first order dependencies to be revealed (Immel et al., 2021) and for the influence of tides and planetary waves to be quantified for the first time (Forbes et al., 2021).

The influence of neutral winds on the plasma motions parallel to the magnetic field at middle and low latitudes is equally challenging to describe because the plasma motions respond to changes in the plasma pressure gradient driven by plasma motion perpendicular to the magnetic field, by changes in ionization production and loss and by collisional momentum exchange between the plasma and the neutral gas. In some instances, when the effects of plasma motions perpendicular to the magnetic field can be minimized and the effects of ionization production and loss can be minimized, relationships between the F-peak height and the F-region wind near the F-peak can be established (Rishbeth, 1967). These techniques can be further refined if the time evolution of the F-peak is known at a given location and a numerical model is utilized to estimate the effects of ion chemistry and plasma motions perpendicular to the magnetic field (Buonsanto et al., 1997). So dominant is the influence of the meridional winds on the F-region peak height that latitude variations in the distribution of the topside plasma density at a fixed altitude can be shown to be strongly correlated with the meridional F-region wind below the peak (Sultan and Rich, 2001). In this study the influence of neutral winds on the topside ionosphere, is revealed directly in seasonal dependencies between the simultaneously measured meridional winds near the F-peak altitude and the interhemispheric flows of plasma observed in the topside at the magnetic equator.

Interhemispheric plasma flows parallel to the magnetic field were first implied by the observation of adiabatic heating and cooling of the plasma in the equatorial region (Hanson et al., 1973). Ionospheric models have been used to demonstrate that the principal drivers of interhemispheric flows in the topside are meridional neutral winds in the lower F region (Bailey and Heelis, 1980) and ion temperature and flows have been observed simultaneously to validate their impact (Venkatraman and Heelis, 1999). More recently, seasonal variations in the interhemispheric flows have been shown to be consistent with changes in the F-peak height, which change the field-aligned plasma pressure gradient across the equator (Burrell and Heelis, 2012). The interhemispheric flows have also been shown to be consistent with the expected behavior of meridional winds near the F-peak derived from an empirical wind model (Drob et al., 2008 ; Burell et al., 2011). Additionally, a longitude dependence in the interhemispheric flows, which is largely driven by the magnetic declination suggests that zonal neutral winds also play a role in the modulation of the interhemispheric flows (Heelis and Hanson, 1980). To date however, simultaneous measurements of the field-aligned interhemispheric plasma flow and the prevailing neutral wind in the F-region have not been made. In this paper we utilize observations from the ICON satellite, which for the first time provide contemporaneous measurements of plasma flows parallel and perpendicular to the magnetic field, the plasma density and the F-region neutral winds at equatorial and middle latitudes. We use this data over the period of 2020 to investigate the seasonal variations in the F-region wind near the F peak and the interhemispheric plasma flow in the topside and the connections between them. We consider two specific local times, one during the daytime and one during the nighttime when the F region is being actively produced by photoionization and when it is decaying under the influence of recombination respectively.

2 Observations.

The ICON spacecraft was launched in 2019 into a low inclination (~27°) circular orbit near 600 km altitude. The instrument payload includes an Extreme Ultra-Violet (EUV) limb imager (Sirk et al., 2017) that provides profiles of the daytime plasma density from 100 km to 500 km on the north limb of the spacecraft orbit (Stephan et al., 2017) and an FUV limb imager (Mende et al., 2017), which provides similar profiles of the nighttime plasma density at the same location (Kalamabadi et al., 2018). The Michelson Interferometer for Global High-resolution Thermospheric Imaging (MIGHTI) (Englert et al., 2017) provides similar altitude profiles of the meridional and zonal winds on the north limb of the satellite orbit (Harding et al., 2017). Finally, the Ion Velocity Meter (IVM) (Heelis et al., 2017) provides a measure of the plasma density and the plasma velocity at the satellite location. In this study, we investigate the relationships between the interhemispheric transport velocity observed at the magnetic equator and the plasma density and wind distribution in the F region at the feet of the magnetic flux tubes near 250 km, that cross the magnetic equator at the satellite altitude of 600 km. Observations as a function of season during the daytime and the nighttime illustrate the role of neutral winds in maintaining hemispheric asymmetries in the plasma density and inducing interhemispheric plasma transport. This work utilizes IVM data version 05, MIGHTI data version 04, EUV data version 03 and FUV data version 04. We do not expect that the results utilizing large-scale seasonal variations studied in this work will be significantly impacted by future improvements to the data products.

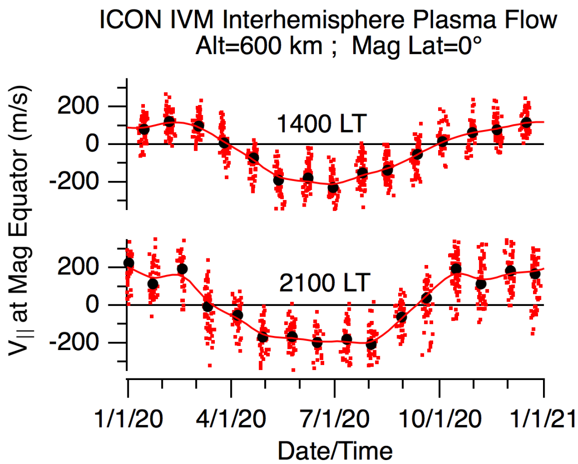

2.1 Topside Plasma Density and Interhemispheric Plasma Flows

Figure 1 shows the seasonal variation in the positive northward interhemispheric plasma flow observed within 1° of the magnetic equator near 600 km altitude. Variations during the year 2020 are shown during the daytime at 1400 LT and during the nighttime at 2100 local time. The local times are chosen to avoid the effects of field-aligned diffusion at the terminators and to eliminate signal contamination from scattered sunlight into the IVM sensor. The data point clusters are approximately 23 days apart, corresponding to the precession period between ascending and descending crossings of the magnetic equator. The point spread within each data cluster encompasses geophysical variability and longitude variations within ± 1 hour of the specified local time and $\pm 1°$ of the magnetic equator. Local time and longitude variations additionally depend on plasma drifts perpendicular to the magnetic field and are a subject for further study. Here, the black dots represent the median values for each equator crossing group and the black curves are a smoothing spline through the medians to illustrate the large-scale seasonal variations of interest. Clearly visible in the seasonal variation is a bulk interhemispheric transport of plasma from the summer to the winter hemisphere induced by a higher flux tube plasma content in the topside summer hemisphere than in the topside winter hemisphere. This difference in the magnetic flux tube plasma content is established during the daytime by photoionization of atomic oxygen and the action of F-region meridional neutral winds that control the height of the F-peak (Rishbeth, 1971). It is retained throughout the night as the F region decays in a manner that preserves the shape of the altitude profile of the O^+ concentration along the magnetic flux tubes. Nighttime interhemispheric flows have a larger magnitude in summer and winter months than during the daytime. However, during the low solar activity conditions prevailing in 2020, the nighttime flux tube content is increasingly influenced by the downward transport of H^+ and more variability in the interhemispheric flow is observed.

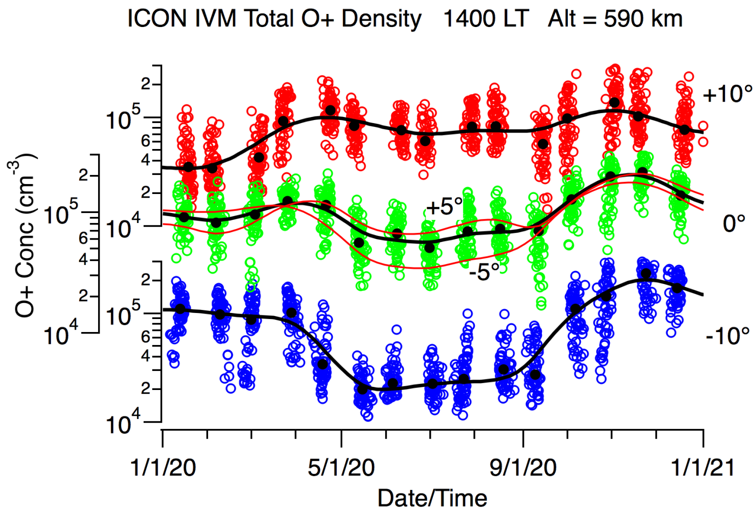

The hemispheric difference in magnetic flux tube plasma content, which drives the interhemispheric flows, is clearly observed in local measurements of the plasma density made by the IVM in the topside. Figure 2 shows the seasonal variations in the topside O^+ density observed at the spacecraft altitude by IVM at 1400 local time during 2020. A similar format to that shown in figure 1 is adopted, with point clusters within 1° at ±10° and at the magnetic equator representing observations at ascending and descending crossings and the solid lines representing a smoothing spline through the median values of each cluster. Also shown by the thin red lines are the smoothed variations at ±5° magnetic latitude. During 2020, the solar activity level is low and in the daytime the satellite resides near the O^+/H^+ transition height. At a fixed altitude in the topside, the O^+ density is elevated on the summer side of the magnetic equator compared to the winter side, in association with a higher F-peak height in summer than in winter produced by the action of meridional winds below the F-peak that are directed from summer to winter. Due to the much larger scale height of H^+ compared to that of O^+, the latitudinal variation along a magnetic flux tube in the equatorial region is much smaller for H^+ than for O^+. Thus, the bulk plasma pressure gradient and the associated field-aligned plasma flow are dominated by the latitude variation in the O^+ density. The O^+ density in the summer hemisphere changes very little between 10° and the magnetic equator. However, it is evident that the O^+ density gradient across the equator is characterized by a large decrease in the O^+ density between the magnetic equator and 10° magnetic latitude in the winter hemisphere. We determine a quantitative measure of the O^+ pressure gradient from a hemispheric asymmetry index defined as $A_s = \frac{(N_{-10}-N_{+10})}{N_{\text{eq}}}$, where the subscripts denote the magnetic latitude of the O^+ density N, at the spacecraft altitude. This index is similar to that utilized by Sultan and Rich (2001). We note that for a fixed local time, samples at the same magnetic latitude in the north and south are displaced in time due to the orbit precession. We thus derive the asymmetry index by utilizing linear interpolation of the smoothing spline through the median values to place them all at the same sample time as the median values at the magnetic equator. The left panels of figure 3 show the strong correlation between the field-aligned interhemispheric plasma flow and the O^+ density gradient across the topside equatorial ionosphere described by the asymmetry index derived at 1400 (upper) and 2100 (lower) local time. The right panels in figure 3 show how the seasonal change in the interhemispheric plasma flow is consistent with changes in the O^+ pressure gradient. As expected, a good correlation remains during the daytime and the nighttime, since the plasma flow in the topside equatorial ionosphere is only influenced by the plasma pressure gradient, which is in turn directly influenced by changes in the F-peak height induced by F-region meridional neutral winds. During the nighttime the dependence of the interhemispheric flow on the O^+ plasma density gradient is weakened by the larger concentrations of H^+ in the topside. However,

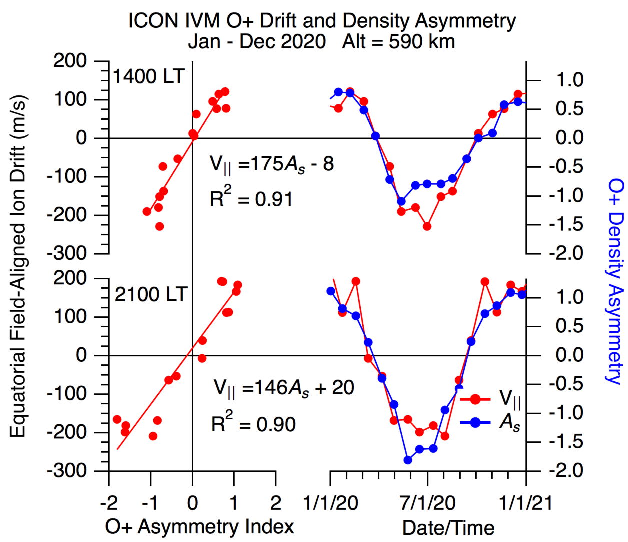

larger hemispheric O^+ density asymmetries and interhemispheric flows appear in the nighttime.

2.2 F-Region Winds and Plasma Density

Unlike previous studies where the response of the F-peak and the topside plasma density is used to deduce the behavior of the F-region neutral wind, the ICON mission is able to simultaneously describe the F-region wind and density that accompanies the plasma behavior in the topside described here. The MIGHTI, EUV and FUV instruments view respectively ±45° and 90° to the satellite orbit plane, with measurements located approximately 13° north of the spacecraft position. By design these measurement locations are near to, or on, the magnetic flux tube that intersects the spacecraft (or equivalently, IVM) when it is at the magnetic equator. Thus, the wind and plasma density profiles at the northern conjugate location are made almost simultaneously with measurements of the interhemispheric plasma flows at the magnetic equator by IVM.

The lower panels of Figure 4 show the horizontal neutral wind in the magnetic meridian at 250 km altitude, extracted from the MIGHTI observations during 2020. To the left are the seasonal variations seen at 1400 local time and to the right are the same variations at 2100 local time. Three rows illustrate the variations seen at +13°, 0° and -13° magnetic latitude. The upper panels repeat the interhemispheric plasma flow in the topside shown in figure 1 to emphasize the similar seasonal variations in the directions of the topside plasma flows and the F-region winds.

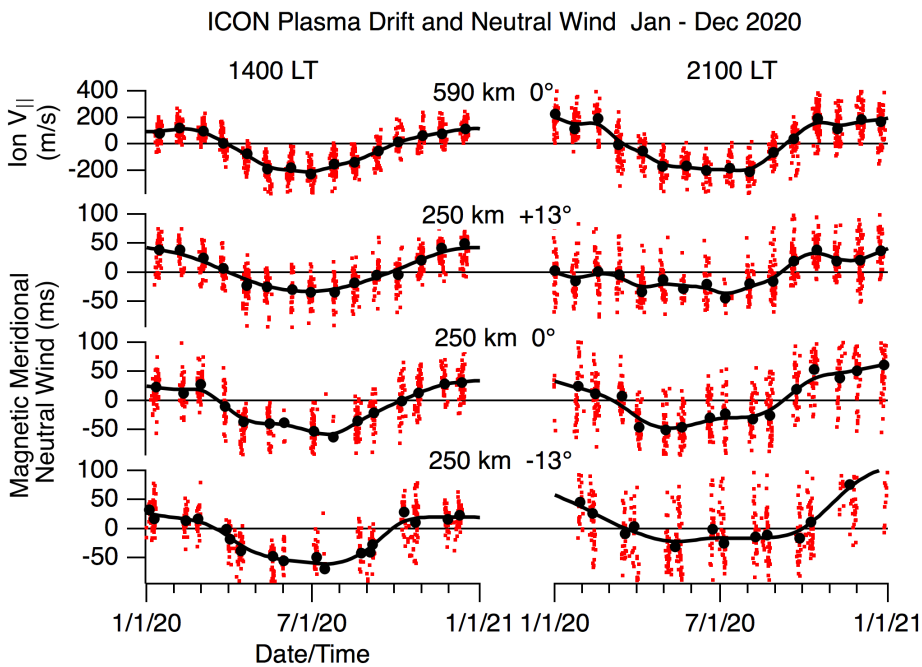

A

similar format to that shown in figure 1 is adopted, with point clusters at $\pm 13°$ and at the magnetic equator representing observations at ascending and descending crossings and the solid lines representing a smoothing spline through the median values of each cluster. Here the contributions of geographic meridional and zonal winds, U_n and U_e respectively, have been resolved in the magnetic meridian to most faithfully represent the vertical forcing of the ionospheric layer by an effective neutral wind expressed as $U^* = U_n \cos\delta + U_e \sin\delta$, where δ is the magnetic declination. A prevailing summer to winter wind is clearly seen during the daytime and the nighttime. However, there are significant differences in the seasonal variations seen during the daytime and nighttime suggesting that both latitude and local time dependencies change with season and solar activity. During the daytime the meridional wind is larger in the winter hemisphere, whereas during the nighttime the opposite is generally true. During the nighttime, the seasonal variation is significantly different at the magnetic equator and at locations north and south of the magnetic equator. The variations are also quite asymmetric as a function of day of the year. These features may indicate a stronger influence of the plasma density on the meridional wind through ion drag, which would additionally be dependent on solar activity. We note that avoidance of the South Atlantic Anomaly and the configuration of the magnetic equator, results in a longitude bias between samples taken at +13° and -13° magnetic latitude which may also contribute to hemispheric asymmetries.

The ICON instrument configuration allows the modulation of the F-peak height produced by the effective meridional wind, to be observed directly from profiles of the daytime and nighttime O^+ density retrieved near ±13° magnetic latitude corresponding to the magnetically conjugate locations of the flux tube that passes through the satellite. Figure 5 shows the seasonal variations in the F-peak height and the F-peak density derived from the EUV instrument at 1400

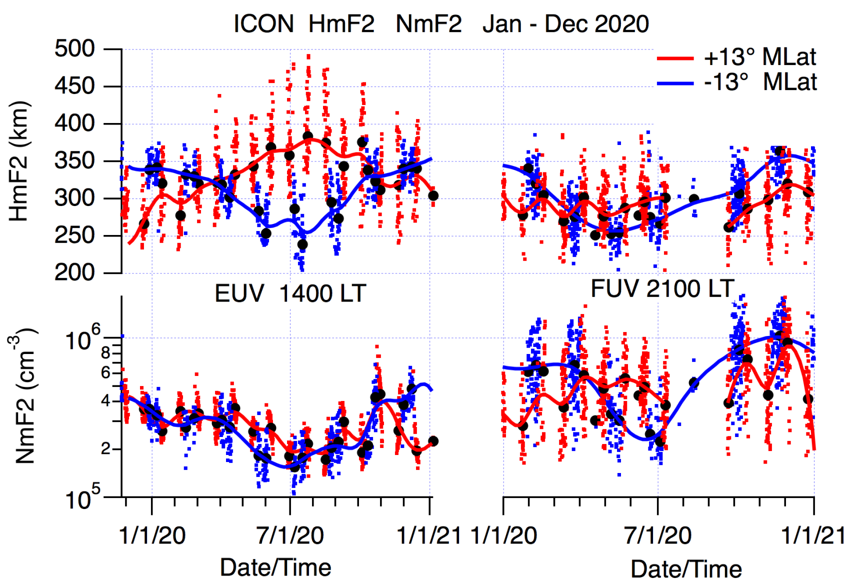

local time and from the FUV instrument at 2100 local time during 2020. As in figure 1, the data clusters represent data gathered during ascending and descending crossings and the solid lines represent a smoothing spline through the median values.

The largest hemispheric asymmetry in the F-peak height is driven by meridional neutral winds below the peak. In northern winter, a south to north wind supports an elevated peak height south of the magnetic equator and a depressed peak height north of the magnetic equator. This behavior is reversed in northern summer. During the daytime, larger hemispheric differences in the peak height are seen in northern summer than in northern winter, consistent with the hemispheric difference in the meridional winds seen in figure 4. We note however, that there are fewer samples at longitudes greater than 230° due to avoidance of the South Atlantic Anomaly and in the southern hemisphere, the longitude coverage is further restricted by the orbit inclination and the instrument viewing geometry. In northern summer, samples are much closer to the sub-solar point at both conjugate locations than in northern winter. During the nighttime the relationship between the F-peak height and the meridional wind is not as robust as seen in the daytime. There is incomplete seasonal coverage available from the FUV instrument but it is clear, by comparing the seasonal variation in figure 4 and 5, that the F-peak height may be additionally influenced by downward plasma drifts perpendicular to the magnetic field, and by downward fluxes of H^+ that charge exchange and produce O^+ to support the maintenance of the F-peak.

The F-peak density is not strongly dependent on the meridional wind. The seasonal variation shown in the lower left panel at 1400 local time clearly describes the seasonal anomaly (e.g. Zeng et al., 2008) and a local increase in solar activity in October and November 2020, interrupts an otherwise small asymmetry in the F-peak density most likely produced by the seasonal difference in solar zenith angle at conjugate locations. The seasonal variation of the O^+ density seen during the daytime is not well preserved at all locations during the nighttime due to the influence of plasma drifts perpendicular to the magnetic field and charge exchange as mentioned previously.

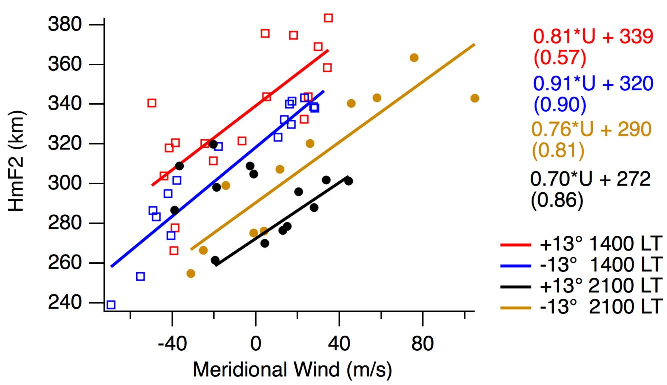

Among the measurements made here, the most direct relationships we may expect are between the interhemispheric plasma flow and the local plasma pressure gradient in the topside shown earlier and between the meridional wind and the F-peak height. The dependence of the F-peak height on the horizontal wind in the magnetic meridian is convolved with additional dependencies of the F-peak height on the time history of the meridional plasma drift perpendicular to the magnetic field and on changes in the O/N_2 ratio, which we assume do not vary significantly as a function of season. To remove short-scale variations in longitude and daily plasma drifts perpendicular to the magnetic field, we consider the relationships between the median values of the F-peak height and the component of the horizontal neutral wind in the magnetic meridian at each crossing of the conjugate latitudes at 1400 and 2100 local time as described in figures 4 and 5. A description of the longitude variations in F-region winds, plasma drifts and densities is deferred to another study. Figure 6 shows the dependence of the F-peak height on the meridional neutral wind in the magnetic meridian near 250 km altitude. Shown separately, for 1400 and 2100 local time are the relationships near +13° and -13° magnetic latitude, corresponding to conjugate locations on the magnetic flux tube through the spacecraft altitude at the magnetic equator. Straight line fits to the data points are used to describe the overall trends. However, as noted earlier the nighttime data are additionally influenced by plasma drifts perpendicular to the magnetic field, which are known to be a function of magnetic activity. Observations taken after October 2020, the time at which solar activity levels increase significantly, are removed from the fitting of the nighttime data but all are shown in figure 6. In the northern hemisphere, the sign of the northward directed neutral wind has been changed to maintain the intuitive relationship between an equatorward directed wind and an increase in F-peak height. We find the F-peak heights at all locations respond to changes in the neutral wind in essentially the same way. The line slopes represent a relationship that is the reciprocal of that derived by Buonsanto (1990) and values between 1 and 1.4 m/s/km are consistent with previously derived values for a dip angle near 65°. In this case the dip angle is approximately 25° but the vertical force applied to the plasma by the meridional wind is about the same, being proportional to $\sin I \cos I$, where I is the dip angle. The point scatter in each hemisphere produces some uncertainty in the F-peak height for zero neutral wind, but any hemispheric difference in the daytime and the nighttime is likely due to differences in the O/N_2 ratio at conjugate locations, which on average lie at higher geographic locations in the north. It should also be recognized that observations at +13° and -13° magnetic latitude are taken during different periods, when the local time history of the meridional (vertical) ExB drift, which affects the F-peak height, will be different for the day of the observation.

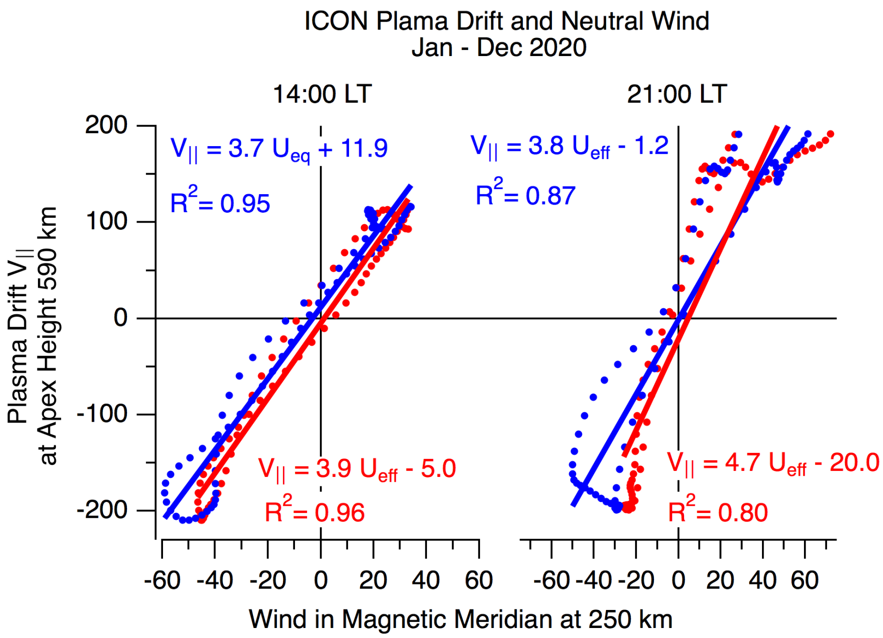

The final relationship we are able to derive for the first time, is that directly observed between the F-region wind below the F-peak near 250 km and the interhemispheric plasma flow across the equator in the topside ionosphere near 600 km. This relationship connects the neutral wind variations shown in figure 4, first to the hemispheric difference in F-peak height, shown in figure 6 and correspondingly to the latitude asymmetry in the plasma distribution in the topside shown in figure 3, and finally to the interhemispheric plasma flow shown in figure 1. The difference in the hemispheric topside plasma content is changed by the field-aligned component of the horizontal neutral wind in the north and the south. Thus, the combined effects of the winds in the north and the south are represented in the average of the horizontal wind in the magnetic meridian at ±13° magnetic latitude and 250 km altitude. Careful examination of the observations at conjugate locations shows that samples are separated by as much as 14 days. We thus use the smoothing spline shown in figure 4 to derive the average wind at ±13° and the interhemispheric plasma flow at the apex height (~600 km) on the same time base with a point every 5 days. Inspection of figure 4 shows that the latitude variation in the meridional wind is quite small and that the neutral wind at the magnetic equator may represent an appropriate proxy for the actions of the winds at ±13°. Figure 7 shows the relationship between the horizontal F-region wind in the magnetic meridian and the interhemispheric plasma flow at the equator derived for the first time from direct measurements of each parameter at 1400 (left panel) and 2100 local time (right panel). Shown here for each local time are two dependencies that are not significantly different. One, shown in red, directly represents the dependence on an effective wind determined from the average of winds near 250 km, at the northern and southern feet of the flux tube through the satellite. The other, shown in blue, is the dependence on only the wind in the magnetic meridian near 250 km altitude at the magnetic equator. In each case a straight-line fit provides a quantitative dependence of the interhemispheric plasma flow at the flux tube apex height on the horizontal wind near the feet of the flux tube at the F peak. We might expect that under daytime conditions, shown in the left panel, when the F-peak is actively maintained by photoproduction and the F-peak height is determined predominantly by the meridional neutral wind, this dependence will remain essentially unchanged. During the nighttime the rate of recombination at and below the F peak is controlled by the meridional wind, which controls the F-peak height as it does during the daytime. However, during the nighttime the topside flux-tube plasma content in the equatorial region is additionally influenced by the plasma drift perpendicular to the magnetic field, which controls the H^+ flux that can charge exchange to make O^+, which subsequently diffuses to lower altitudes to support the F-peak density. This gives rise to a more variable relationship between the F-region meridional wind and the interhemispheric plasma flow at the magnetic flux tube apex, which is shown in the right panel of figure 7. As for the daytime, the relationships between the interhemispheric plasma flow and the neutral wind are shown for an effective wind, being the average of the winds at the northern and southern feet and the trans-equatorial wind at the magnetic equator. Despite the additional variability we find that the neutral wind control of the F peak height dominates the topside field-aligned plasma pressure gradient and that the relationship between the trans-equatorial wind and the interhemispheric plasma flow remains essentially unchanged.

3 Discussion

The influence of F-region neutral winds on the plasma flows parallel to the magnetic field in the topside is one of the more direct signatures of ion-neutral interactions in the ionosphere-thermosphere system. With models of these interactions and observations from the ground, we are able to verify directly that the F-peak height at middle and low latitudes is dominated by winds in the magnetic meridian near the F peak (Richards, 1991). Using these well-established relationships, the global behavior of the wind can be specified (Dandenault , 2018). The relationships between the wind and plasma dynamics parallel to the magnetic field is less well established since the connections depend upon the magnetic flux tube apex height, the magnetic latitude at which the wind is specified and the local time.

The ICON mission has provided measurements that for the first time establish the observed relationship between these parameters. Here the changes in the F-region horizontal wind in the magnetic meridian are produced by a prevailing summer to winter trans-equatorial wind with seasonal variations that are comparable to or larger than the daily variation. Thus, we contrast the behavior during the daytime at 1400 LT and during the nighttime at 2100 LT when the prevailing trans-equatorial wind is about the same during the same season. In both cases a wind in the magnetic meridian plane serves to raise and lower the F-peak height and thus change the O^+ loss rate. During the daytime, wind-induced changes in the F-peak height are accompanied by increases or decreases in both the photoproduction rate and the loss rate, such that changes in the F-peak density are largely unchanged except for seasonal changes in the O/N_2 ratio which describe the seasonal anomaly. However, the prevailing horizontal wind in the magnetic meridian raises the F-peak in the summer hemisphere and lowers it in the winter hemisphere at magnetic latitudes below the subsolar latitude, most of which are accessible by ICON instruments except for the limb instruments at southern magnetic latitudes and longitudes between 200° and 300°. At magnetic latitudes of 13° the magnetic inclination is sufficient to sensibly derive a relationship between changes in the neutral wind and the F-peak height, with dependencies similar to those extracted using a servo model. More importantly, the relationship between the interhemispheric plasma flow and the topside latitudinal plasma density gradient can be specified with high confidence. In the topside equatorial ionosphere, where O^+ is the major ion species we might expect that O^+ will evolve preserving the same altitude distribution at all times, since the O^+ loss rate is linearly proportional to the O^+ density. This would produce essentially the same relationship, during the daytime and the nighttime, between the interhemispheric plasma flow and the latitude gradient in O^+ density at a fixed altitude. We find a small day-night difference in this relationship, but also note that during the prevailing solar minimum conditions O+ decays as expected while H^+ is transported downward and contributes an additional source of O^+ through charge exchange (Huba et al, 2021).

Since the latitudinal plasma density gradient is directly dependent on the hemispheric difference in the F-peak height on a flux tube, the relationship between the neutral wind in the magnetic meridian and the interhemispheric plasma flow at the apex height is also derived with high confidence. Within about 15° of the magnetic equator we find that the prevailing meridional neutral wind has a small latitude gradient. Thus, the wind at the magnetic equator may serve almost the same function as the hemispheric difference in the wind at the northern and southern feet of the flux tube. Indeed, we find that for a magnetic apex height near 600 km the interhemispheric transport velocity is about 4 times the trans-equatorial wind speed.

The effectiveness of the meridional wind in raising and lowering the F-peak is dependent on the magnetic inclination I as $\cos I \sin I$. Thus, we expect that in the low latitude region where the wind across the equator is a good proxy for the winds at the flux tube feet, the linear coefficient may vary similarly with latitude. Despite the expectation that the relationship between the F-peak height and the meridional wind will vary with magnetic inclination, the relationship between the wind and the interhemispheric plasma transport velocity at the apex height will quickly break down at apex heights for which charge exchange and field-aligned transport of H^+ become more important to the O^+ distribution. This is particularly applicable at during solar minimum at night , when the O^+/H^+ transition height falls to altitudes below 500 km. In addition we note that the fidelity with which the meridional wind at the magnetic equator can be used as a proxy for the average of the meridional wind at the flux tube footpoints, is reduced as the magnetic field apex height increases.

Acknowledgments

ICON is supported by NASA's Explorers Program through contracts NNG12FA45C and NNG12FA42I. The data utilized in this study are available at the ICON data center (https://icon.ssl.berkeley.edu/Data). The authors would like to thank Tori Fae and the ICON Science Operations Center for diligently maintaining the ground processing procedures.

References

Bailey, G,J. and R.A. Heelis (1980), Ion temperature troughs induced by a meridional neutral air wind in the night-time equatorial topside ionosphere, Planetary and Space Science,28, 895-906.

Buonsanto, M. J., Starks, M. J., Titheridge, J. E., Richards, P. G., and Miller, K. L. (1997), Comparison of techniques for derivation of neutral meridional winds from ionospheric data, *J. Geophys. Res.*, 102(A7), 14477– 14484, doi:10.1029/97JA01149.

Burrell, A. G., R. A. Heelis, and R. A. Stoneback (2011), Latitude and local time variations of topside magnetic field-aligned ion drifts at solar minimum, J. Geophys. Res., 116, A11312, doi:10.1029/2011JA016715.

Burrell, A. G., and R. A. Heelis (2012), The influence of hemispheric asymmetries on field-aligned ion drifts at the geomagnetic equator, Geophys. Res. Lett., 39, L19101, doi:10.1029/2012GL053637.

Dandenault, P. B. (2018). MENTAT: A new wind model for Earth's thermosphere.Journal of Geophysical Research: Space Physics,123, 7124–7147.https://doi.org/10.1029/2018JA025551

Drob, D., et al. (2008), An empirical model of the Earth's horizontal wind fields: HWM0, J. Geophys. Res., 113, A12304, doi:10.1029/2008JA013668.

Englert, C.R., Harlander, J.M., Brown, C.M., Marr, K.D., Miller, I.J., Stump, J.E., Hancock, J., Peterson, J.Q., Kumler, J., Morrow, W.H., Mooney, T.A., Ellis, S., Mende, S.B., Harris, S.E., Stevens, M.H., Makela, J.J., Harding, B.J., and Immel, T.J., (2017), Michelson Interferometer for Global High-resolution Thermospheric Imaging (MIGHTI): instrument design and calibration. Space Science Reviews, 212(1-2), pp.553-584. DOI: 10.1007/s11214-017-0358-4

Forbes, J. M., Zhang, X., Heelis, R., Stoneback, R., Englert, C. R., Harlander, J. M., et al. (2021). Atmosphere-Ionosphere (A-I) coupling as viewed by ICON: Day-to-day variability due to planetary wave (PW)-tide interactions. *Journal of Geophysical Research: Space Physics*, 126, e2020JA028927. https://doi.org/10.1029/2020JA028927.

Hanson, W. B., Nagy, A. F., and Moffett, R. J. (1973), Ogo 6 measurements of supercooled plasma in the equatorial exosphere, *J. Geophys. Res.*, 78(4), 751–756, doi:10.1029/JA078i004p00751.

Harding, B.J., Makela, J.J., Englert, C.R., Marr, K.D., Harlander, J.M., England, S.L. and Immel, T.J., (2017). The MIGHTI Wind Retrieval Algorithm: Description and Verification. Space Science Reviews, 212(1-2), pp.585–600. DOI: 10.1007/s11214-017-0359-3

Heelis, R.A., Stoneback, R.A., Perdue, M.D., Depew, M.D., Morgan, W.A., Mankey, M.W., Lippincott, C.R., Harmon, L.L., and Holt, B.J., (2017). Ion Velocity Measurements for the Ionospheric Connections Explorer. Space Science Reviews, 212(1-2), pp.615-629, DOI: 10.1007/s11214-017-0383-3

Heelis, R., and Hanson, W. (1980), Interhemispheric transport induced by neutral zonal winds in the *F* region, *J. Geophys. Res.*, 85(A6), 3045– 3047, doi:10.1029/JA085iA06p03045.

Heelis, R. A., Coley, W. R., Burrell, A. G., Hairston, M. R., Earle, G. D., Perdue, M. D., Power, R. A., Harmon, L. L., Holt, B. J., and Lippincott, C. R. (2009), Behavior of the O+/H+ transition height during the extreme solar minimum of 2008, *Geophys. Res. Lett.*, 36, L00C03, doi:10.1029/2009GL038652.

Huba, J.D., R.A. Heelis and A. Maute (2021) Large-scale O+ Depletions Observed by ICON in the Post-Midnight Topside Ionosphere: Data/Model Comparison *Geophysical Research Letters*, *48,7* https://doi.org/10.1029/2020GL092061

Immel, T.J., S.L. England, S.B.Mende, R.A. Heelis, et al. (2018) The Ionospheric Connection Explorer mission: Mission goals and design. Space Sci Rev (2018) 214: 13. https://doi.org/10.1007/s11214-017-0449-2

Immel, T., B.J. Harding, R.A. Heelis, A. Maute, J. Forbes, S.L. England, S.B. Mende, C.R. Englert, R.A. Stoneback, K. Marr, J.M. Harlander and J.J. Makela (2021) Control of ionospheric plasma velocities by thermospheric winds, *Nat. Geosci.* **14,** 893–898 (2021). https://doi.org/10.1038/s41561-021-00848-4

Kamalabadi, F., Qin, J., Harding, B.J., Iliou, D., Makela, J.J. Meier, R.R., Englans, S.L., Frey, H.U., Mende, S.B. and Immel, T.J. (2018), Inferring nighttime ionospheric parametes wit the Far Unltravilolet Image onbaoard the Ionospheric Commection Explorer, Space Science Review, 214:60 (14pp.) Public Access. doi: 10.1007/s11214-018-0502-9.

Maute, A., Richmond, A. D., and Roble, R. G. (2012), Sources of low-latitude ionospheric $\mathbf{E} \times \mathbf{B}$ drifts and their variability, *J. Geophys. Res.*, 117, A06312, doi:10.1029/2011JA017502.

Mende, S.B., Frey, H.U., Rider, K., Chou, C., Harris, S.E., Siegmund, O.H.W., England, S.L., Wilkins, C., Craig, W., Immel, T.J. and Turin, P. (2017), The far ultra-violet Imager on the ICON mission. Space Science Reviews, 212(1-2), pp.655-696, DOI: 10.1007/s11214-017-0386-0

Richards, P. G. (1991), An improved algorithm for determining neutral winds from the height of the F_2 peak electron density, *J. Geophys. Res.*, 96(A10), 17839– 17846, doi:10.1029/91JA01467.

Rishbeth, H. (1967), The effect of winds on the ionospheric F2-peak, J. Atmos. Terr. Phys., 29, 225–238.

Sirk, M. M., Korpela, E. J., Ishikawa, Y., Edelstein, J., Wishnow, E. H., Smith, C., McCauley J., McPhate J.B., Curtis J., and Gibson, S. R., (2017). Design and performance of the ICON EUV spectrograph. Space Science Reviews, 212(1-2), pp.631-643. doi: 10.1007/s11214-017-0384-2

Stephan, A.W., Korpela, E.J., Sirk, M.M., England, S.L. and Immel, T.J., (2017). Daytime Ionosphere Retrieval Algorithm for the Ionospheric Connection Explorer (ICON). Space Science Reviews, 212(1-2), pp.645-654, DOI: 10.1007/s11214-017-0385-1

Sultan, P.J. and F.J. Rich (19Sultan, P. J., and Rich, F. J. (2001), Determination of a proxy for F region meridional neutral winds using in situ satellite ion density measurements, *J. Geophys. Res.*, 106(A10), 21033– 21038, doi:10.1029/2000JA000219.

Venkatraman, S., & Heelis, R. (1999). Effects of solar activity variations on adiabatic heating and cooling effects in the nighttime equatorial topside ionosphere. Journal of Geophysical Research, 104(A8), 17,117–17,126. https://doi.org/10.1029/1999JA900196.

Zeng, Z., Burns, A., Wang, W., Lei, J., Solomon, S., Qian, L., et al. (2008). Ionospheric annual asymmetry observed by the cosmic radio occultation measurements and simulated by the TIEGCM. Journal of Geophysical Research, 113, A07305. https://doi.org/10.1029/2007JA01289